Theoretical Chemistry Accounts (2018) 137:126
https://doi.org/10.1007/s00214-018-2307-z

REGULAR ARTICLE

A systematic electronic structure study of the O–O bond dissociation energy of hydrogen peroxide and the electron affinity of the hydroxyl radical

Danilo J. Carmona[1] · David R. Contreras[2] · Oscar A. Douglas-Gallardo[1] · Stefan Vogt-Geisse[1] · Pablo Jaque[3] · Esteban Vöhringer-Martinez[1]

Received: 1 June 2018 / Accepted: 22 August 2018 / Published online: 12 September 2018

Abstract

Hydroxyl radical reduction and peroxide bond breaking in hydrogen peroxide are reactions involved in various processes such as the Fenton reaction, which has applications as e.g. groundwater remediation. Here, we study these two reactions from a thermodynamical point of view through the bond dissociation energy (BDE) of the O–O bond in hydrogen peroxide and the electron affinity (EA) of the hydroxyl radical. High-level ab-initio calculations at the complete basis set (CBS) limit were carried out, and the performance of different DFT-based methods was addressed by following a specific classification on the basis of the Jacob's ladder in combination with various Pople's basis sets. The ab-initio calculations at the CBS limit are in agreement with experimental reference data and identify a significant contribution of the electron correlation energy to the BDE and EA. The studied DFT-based methods were able to reproduce the ab-initio reference values, although no functional was particularly detected as the best for both reactions. The inclusion of certain percentage of Hartree–Fock (HF) exchange in DFT functionals leads in most cases to smaller BDE and EA values, which might be related to the poor description of the two reactions by the HF method. Considering the computational cost, DFT methods provide better BDE and EA values than HF methods with an accuracy comparable to the MP2 or CCSD level of theory. Additionally, the quality of the hydrogen peroxide, hydroxyl radical and hydroxyl anion structures obtained from these functionals was compared to experimental reference data. In general, bond lengths were well reproduced and the errors in the angles were between one and two degrees with some systematic trend with respect to the basis set's size. From our results we conclude that DFT methods present a computationally less expensive alternative to describe these two reactions that play a role in the Fenton reaction. The benchmark that is carried out in this study provides a systematic validation of various approximated $E_{xc}[\rho]$ functionals combined with different basis sets, which could serve as a stepping-stone for future research on the Fenton reaction.

Keywords Hydrogen peroxide · DFT · CBS limit · BDE · Electron affinity

Electronic supplementary material The online version of this article (https://doi.org/10.1007/s00214-018-2307-z) contains supplementary material, which is available to authorized users.

✉ Esteban Vöhringer-Martinez
evohringer@udec.cl

Pablo Jaque
pablo.jaque@ciq.uchile.cl

[1] Departamento de Físico-Química, Facultad de Ciencias Químicas, Universidad de Concepción, Concepción, Chile

[2] Departamento de Química Analítica e Inorgánica, Facultad de Ciencias Químicas, and Centro de Biotecnología, Universidad de Concepción, Concepción, Chile

[3] Departamento de Química Orgánica y Fisicoquímica, Facultad de Ciencias Químicas y Farmacéuticas, Universidad de Chile, Sergio Livingstone 1007, Independencia, Santiago, Chile

1 Introduction

The capability of hydrogen peroxide to produce hydroxyl radicals in aqueous solution due to the catalytic effect of metal cations is widely known [1]. In biological systems, hydroxyl radical is partly responsible for protein inactivation, breaking of cell membranes, genotoxicity and other phenomena related to cell damage owing to its degradative properties [2]. The same process has also been used for industrial purposes such as in the Fenton reaction [3], where water contaminants are degraded by hydroxyl radicals generated through the Fe^{2+}-assisted reductive cleavage of an O–O bond in hydrogen peroxide:

$$Fe^{2+}(aq) + H_2O_2(aq) \rightarrow Fe^{3+}(aq) + \cdot OH(aq) + OH^-(aq) \quad (1)$$

Research on is kind of reactions has been mainly focused on improving its performance at industrial scale. For example, Fenton processes (Eq. 1) can be modified by changing the reaction conditions (pH, temperature, etc.) and the nature of the reactants (e.g. considering other reducing metal centers) or by induction of the peroxide bond breaking through light (photo-Fenton processes) or sound waves irradiation (sono-Fenton processes), and by the assistance of peroxide reduction using electrolysis (electro-Fenton processes) [1]. However, a rigorous theoretical study about the thermodynamic determining factors of these reactions has not been done to our knowledge. In principle, such description could be achieved on the basis of a characterization of the electronic structure of reactants and products, which would facilitate a physical interpretation. If a predictive point of view would be achieved from first principles, then a reduced number of experiments would be necessary to obtain better conditions to perform, for example, Fenton processes.

High computational cost and sometimes low accuracy are natural disadvantages arising when a deeper theoretical description of complex chemical systems is intended. Two approaches can contribute to fix these difficulties: the first one is the use of a highly approximated method to describe the system. In this case, the computational cost is reduced but the accuracy and overall the physical interpretation are sacrificed. The second way corresponds to the exclusion of some variables of the system (presence of solvent, pH, temperature etc.), which facilitates a physical insight, but is sometimes far from the real conditions. Following the latter approach, determining factors of the Fenton reaction can be classified into intrinsic and extrinsic types: the former factors affect the reactants and products interacting in an isolated way, while the latter ones include everything else involved in the reaction, for example, solvent effects, nature of ligands that coordinate to the metal center, temperature, etc. In this first systematic study we mainly focus on the intrinsic factors for a theoretical description of the hydroxyl radical reduction and peroxide bond dissociation in hydrogen peroxide, which are reactions related to Fenton processes. This description is made by using a set of both high-level ab-initio and density functional theory (DFT) methods.

In order to perform a systematic study of the intrinsic factors of the Fenton reaction, the overall process can be thought from a purely thermodynamical point of view as composed by three reactions: the first one corresponds to the divalent iron oxidation. The other two involve the energy changes associated with the hydrogen peroxide molecule: homolytic peroxide bond breaking (PBB) and hydroxyl radical reduction (HRR):

$$\begin{aligned} &H_2O_2 \rightarrow 2{\cdot}OH && \text{Homolytic peroxide bond breaking (PBB)} \\ &{\cdot}OH + e^- \rightarrow OH^- && \text{Hydroxyl radical reduction (HRR)} \end{aligned} \tag{2}$$

Since Fenton processes have also been reported for other metal cations being different from iron [1], here we mainly focused on both reactions: PBB and HRR. To describe these two reactions assuming isolated reactants and products, we use electronic structure methods and compare our results with experimental data to evaluate the performance of each approach. The experimental parameter characterizing the PBB step is the homolytic bond dissociation energy (BDE), which corresponds to the standard enthalpy difference associated to the reaction in gas phase at 298.15 K [4]:

$$\mathrm{BDE} = 2\Delta_f H^0_{298.15}({\cdot}\mathrm{OH}) - \Delta_f H^0_{298.15}(\mathrm{H_2O_2}) \tag{3}$$

For the HRR step, the associated experimental observable is the electron affinity (EA) of the hydroxyl radical, which is the energy released in the reduction of hydroxyl radical in gas phase at 0 K [5]:

$$\mathrm{EA}({\cdot}\mathrm{OH}) = -[\mathrm{E}(^-\mathrm{OH}) - \mathrm{E}({\cdot}\mathrm{OH})] \tag{4}$$

Although BDE and EA are measured in conditions very far from the reality of Fenton reaction, we can take advantage of the availability of experimental data for these parameters to validate an electronic structure calculation method suitable of providing additional information about the Fenton reaction in general. Wave function theory (WFT)-based methods arise as a good choice at first glance because hydrogen peroxide and hydroxyl radical are small molecules able to be computationally studied at a high level of theory. However, description of other aspects to model the Fenton reaction will require the consideration of more realistic conditions as the inclusion of electronic structure calculations for transition metals and solvent effects, which impede the usage of computationally expensive post-HF methods. In this context, DFT methods present a suitable alternative because some exchange-correlation functionals have shown good performance in electronic structure calculations for transition metal-containing systems in a wide range of conditions after they have been tested [6, 7]. A systematic DFT-based benchmark of PBB and HRR constitutes, therefore, a good starting point for a complete theoretical modeling of the Fenton reaction.

The DFT benchmark was based on a thorough choice of the E_{xc} functional and basis set, because these factors determine the performance of the electronic energy calculations within the Kohn–Sham framework of DFT [25–28]. E_{xc} functionals can be systematically classified by inter alia the following criteria: Jacob's ladder rung [29, 30], Hartree–Fock exchange percentage [31, 32], inclusion of a range separation function [33, 34], and the consideration of empirical fitting when designing the functional. Table 1 shows a representative set of functionals used in this study and their classification using these criteria. Additionally, their mean unsigned errors (MUEs) for both BDE and EA for

Table 1 Chosen DFT- and WFT-based methods and their features (MUE in kcal mol^{-1})

Method	MUE for BDE[a]	MUE for EA[a]	Jacobs Ladder rung	%HF exc.[b]	Range separated	Semi-empirical	References
N12	5.63	4.21	GGA	0	NO	YES	[8]
BLYP	11.66	2.68	GGA	0	NO	YES	[9, 10]
PBE	6.14	2.27	GGA	0	NO	NO	[11]
MN12L	4.85	2.65	mGGA	0	NO	YES	[12]
M06-L	7.75	3.83	mGGA	0	NO	YES	[13]
B3LYP	9.84	2.33	HGGA	20	NO	YES	[9, 10, 14]
PBE0	7.12	2.79	HGGA	25	NO	NO	[15]
SOGGA11-X	4.97	1.55	HGGA	40	NO	YES	[16]
ωB97	3.85	2.58	HGGA	0–100[c]	YES	YES	[17]
ωB97-X	4.45	2.01	HGGA	15–100[c]	YES	YES	[17]
ωB97-XD	4.52	1.86	HGGA	22–100[c]	YES	YES	[18]
BMK	3.78	1.61	HmGGA	42	NO	YES	[19]
M06	4.10	1.85	HmGGA	27	NO	YES	[13]
M06-2X	2.50	2.14	HmGGA	54	NO	YES	[13]
M05-2X	2.64	2.04	HmGGA	56	NO	YES	[20]
M11	3.13	0.89	HmGGA	43–100[c]	YES	YES	[21]
HF	36.26	26.98	WFT	100	NO	NO	[22]
MP2	4.80	3.02	WFT	100	NO	NO	[23]

[a]From Peverati and Truhlar database [24]. MG3S basis set was used; [b]for hybrid functionals; [c]short and long range %HF exchange, respectively

the respective database investigated by Peverati and Truhlar were added [24]. These different functionals are then combined with basis sets that can be modulated by adding diffuse-type functions (Gaussians with a smaller exponent), splitting a valence–shell's basis set into more than one, i.e. from double-ζ to triple-ζ basis sets, or adding Gaussian-type orbitals of a different angular moment (also called polarization-type functions). We decided to stick to Pople's basis set including all these variations since some semi-empirical DFT functionals have been parameterized with these basis sets [24]. Finally, the DFT benchmark was validated by high-level ab-initio calculations at the CBS limit and compared to experimental data.

Table 2 Experimental data for BDE, EA and geometrical parameters of the involved species

Parameter	Value	References
BDE (kcal mol^{-1})	50.35 ± 0.10	[4]
EA (kcal mol^{-1})	42.147	[35]
R(O–H) (Å)	0.9697[a]	[36]
R(O–H) (Å)	0.964[b]	[37]
R(O–O) (Å)	1.461[d]	[38]
R(O–H) (Å)	0.9675[c,d]	[38]
A(O–O–H) (°)	100.07[d]	[38]
D(H–O–O–H) (°)	119[d]	[38]

[a]For hydroxyl radical, [b]For hydroxyl anion, [c]for hydrogen peroxide, [d]ab initio corrected, see reference [38]

2 Methods

Experimental reference values for BDE, EA and geometrical parameters of hydrogen peroxide, hydroxyl radical and hydroxyl anion were considered in this work and are summarized in Table 2.

Reference values for electronic BDE (eBDE, electronic energy change associated to the PBB process; Eq. 2) and EA were also obtained with high-level ab-initio methods. These parameters were computed at a complete basis set (CBS) limit at the CCSDT(Q) level. Extrapolations were performed by considering Dunning's basis sets up to quintuple-ζ quality (except for CCSDT and CCSDT(Q) levels, where only double- and triple-ζ qualities were considered). In order to produce a reliable description of the anionic state in the case of EA, these basis sets were augmented with diffuse-type functions. Experimental geometries of the involved species (Table 2) were considered through all the calculations using the PSI 4 program [39] coupled to the MRCC suite [40].

Assessment of DFT-based methods was performed in the following way: geometry optimizations and frequency calculations of hydrogen peroxide, hydroxyl radical and hydroxyl anion were carried out in order to confirm minimum energy structures on the potential energy surfaces (zero imaginary frequencies) and to obtain formation enthalpies of these species. Values of BDE, EA (Eqs. 3 and 4) and geometrical parameters of the involved species were calculated for each

DFT method from the obtained structures and then compared to the reference values shown in Table 2. All these calculations were carried out using the *Gaussian 09* package of programs [41].

Following criteria were taken into account for the choice of density functionals in the present study: (1) their performance in the reproduction of physical properties in two databases used by Peverati and Truhlar in 2014 [24]: ABDE12 database includes R–X bond dissociation energies in small organic molecules, where R = methyl, ethyl, isopropyl or tert-buthyl, and X = hydrogen, methyl, methoxy or hydroxy; and EA13/03 database comprises electron affinities of six main-group atoms (C, S, O, P, Si and Cl) and seven small molecules including the hydroxyl radical (SH, Cl_2, OH, O_2, PH, PH_2 and S_2); (2) they covered all rungs of the Jacob's ladder, (3) the parameters (semi-empirical and non-empirical) considered in the functional's parametrization, and (4) range separation exchange-correlation functionals were also included. Detailed description of the chosen functionals can be found in Table 1. Additionally, two wavefunction-based methods (HF and MP2) were also tested with the basis sets depicted in the following paragraph.

The effect of the basis set was tested by comparing four Pople's basis sets, which may determine the flexibility of the electron density (i.e. homogeneity vs. non-homogeneity of the electron density). MG3S basis set (6-311+G(2df,2p)) [42] was the starting point because this was used in the databases of Peverati and Truhlar [24]. To reduce the computational cost the 6-31G(d,p) basis set was considered and then by successively adding diffuse functions and splitting the valence one arrives to the 6-31+G(d,p) and 6-311+G(d,p) basis sets, respectively. The MG3S basis set is obtained by adding polarization functions to the lastly considered set. Only basis sets including diffuse functions were considered for the reaction including the hydroxyl anion [43].

Performance of each combination of DFT-based functional and basis set was given by the computation of signed and unsigned errors (SE and UE, respectively):

$$\mathrm{SE} = \text{Calculated value} - \text{Reference value} \quad \mathrm{UE} = |\mathrm{SE}| \tag{5}$$

3 Results and discussion

3.1 Bond dissociation energy of the oxygen–oxygen bond in hydrogen peroxide

We analyze the peroxide bond breaking in hydrogen peroxide as the first reaction related to Fenton processes through the calculation of the bond dissociation energy (BDE) of its oxygen–oxygen bond. To obtain a reference value for the electronic energy of this reaction we used high-level ab-initio methods together with complete basis set extrapolation. The results are summarized in Table 3 for the Dunning's basis set up to quintuple-ζ with electron correlation energy corrections of up to CCSDT(Q). The eBDE are poorly estimated by HF level of theory due to lack of Coulomb-type correlation, which is crucial for a proper description of homolytic eBDE. This becomes evident when observing the correlation energy correction at the MP2 level of theory which amounts to 64.80 kcal mol^{-1} at the CBS limit. However, the MP2 energy still does not provide an accurate estimate of the eBDE because it overestimates the energy by almost 10 kcal mol^{-1}. These effects are also observed when the decomposition of hydrogen peroxide in molecular oxygen and molecular hydrogen (which does not consider radicallary species) is considered (Table S.1, supporting information). Therefore, the inclusion of higher rank excitations (up to CCSDT) are paramount to obtain a result of chemical accuracy. The eBDE computed at the CCSDT(Q)/CBS amounts to 55.16 kcal mol^{-1} (Table 3). Adding DFT calculated zero point energy and enthalpy corrections under the rigid rotor and harmonic oscillator approximations, results in a BDE value ranging from 50.34 to 51.06 kcal mol^{-1} (depending on the DFT functional used to obtain frequencies and moments of inertia as shown in Table S.2 of the supporting information). This value is in very good agreement with the experimental value of 50.35 kcal mol^{-1} (Table 2). The highly correlated ab initio eBDE provides a reliable benchmark energy upon which a myriad of different DFT functionals will be compared.

To address systematic deviations of the different functionals we first calculated the signed error (SE) between the

Table 3 Contributions to the electronic BDE at various level of theory and basis sets and extrapolated to the CBS limit

eBDE (kcal mol^{-1})	SCF	MP2-SCF	CCSD-MP2	CCSD(T)-CCSD	CCSDT-CCSD(T)	CCSDT(Q)-CCSDT	Correlated BDE
cc-pvdz	− 1.68	54.97	− 9.65	3.47	− 0.08	0.56	47.05
cc-pvtz	− 0.90	61.27	− 12.59	5.09	− 0.39	0.57	52.48
cc-pvqz	− 1.47	63.06	− 13.27	5.41	–	–	53.74
cc-pvQz	− 1.69	63.91	− 13.50	5.54	–	–	54.26
CBS limit	− 1.74	64.80	− 13.74	5.66	− 0.39	0.57	55.16

electronic BDE calculated at the DFT level and the ab-initio reference value obtained above. Comparison of these values among the considered functionals shows a systematic behavior for the different basis sets. SE values decrease conform the basis set size is augmented from 6-31G(d,p) to 6-311+G(d,p) (inserted graphic in Fig. 1). Addition of more d- and f-polarization functions on oxygen atoms and p-polarization functions on hydrogen atoms in 6-311+G(d,p) to obtain the MG3S basis set results in an increasing of the SE values (see Figure S.1 in supporting information). Trend in bond dissociation electronic energy can be explained in terms of differences in the description of hydrogen peroxide and hydroxyl radical (reactant and products, respectively). When the basis set size is augmented, the electronic energy always decreases in all the involved species. It can be easily shown that SE only becomes smaller when the total electronic energy decreasing in products is higher than in reactants. Therefore, the hydroxyl radical is most sensible

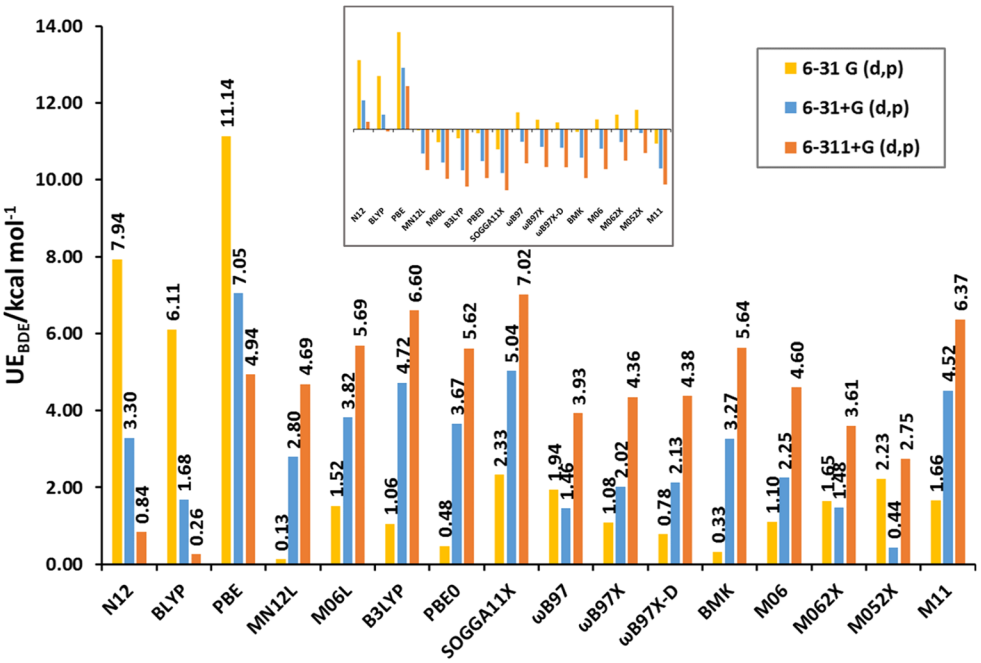

Fig. 1 Unsigned error (UE) for DFT calculated BDE values with regard to the ab-initio reference in kcal mol^{-1}. Inserted graphic shows the sign of the corresponding signed error (SE) values

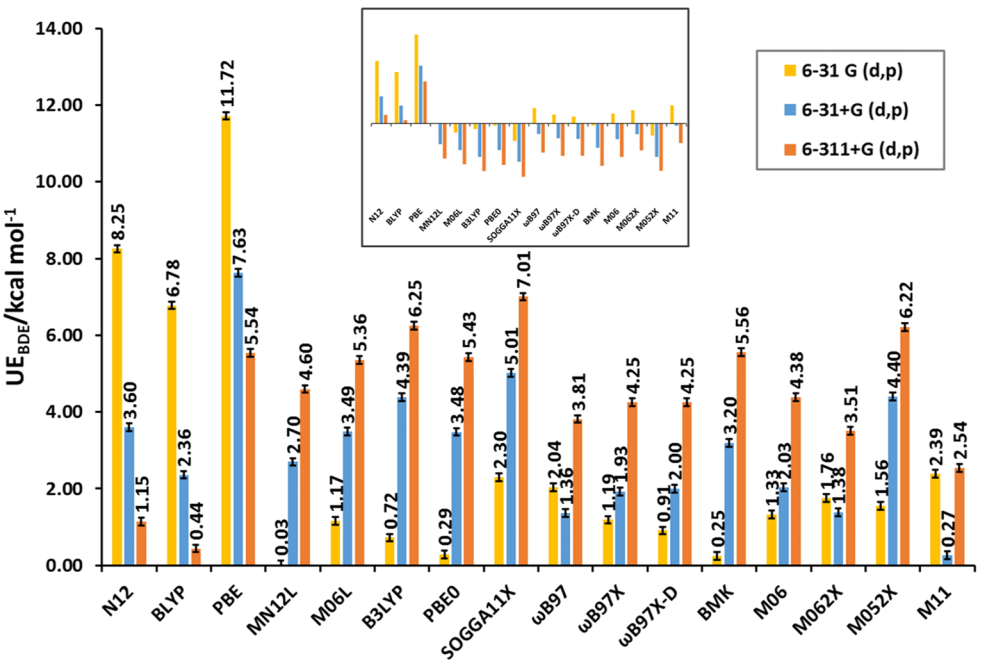

Fig. 2 Unsigned error (UE) for DFT calculated BDE values with regard to the experimental reference in kcal mol^{-1}. Error bars show the experimental error of 0.10 kcal mol^{-1} (Table 2). Inserted graphic shows the sign of the corresponding signed error (SE) values

to the increasing of the basis set size. However, this conclusion cannot be generalized since most functionals are mainly designed to reproduce chemical properties derived from energy differences instead of absolute electronic energies (Table 1).

Therefore, deviation of DFT functionals from the ab-initio reference value is better studied by the unsigned errors (UE) that ranged between 0.13 and 11.14 kcal mol^{-1}. Only 12 of the 64 methods yielded an UE value higher than 5 kcal mol^{-1}, which ascribes the resting 52 combinations of DFT functional and basis sets an error comparable to the 0.03 to 3.89 kcal mol^{-1} found for MP2 calculations with these basis sets (see Figure S.1 in supporting information). HF method yields UE values above 50 kcal mol^{-1} for the Pople's basis sets, which is in agreement with the ab-initio calculations discussed above that identified electron correlation as key contribution to obtain correct bond dissociation electronic energies. Interestingly, DFT-based methods are able to improve HF results considerably by accounting for electron correlation, although not in a systematic way which would allow an extrapolation to converged values.

Comparison of the different DFT methods in Fig. 1 shows that the dependence of the UE values when going from 6-31G(d,p) to 6-311+G(d,p) basis set differs for two categories. GGA functionals (N12, BLYP and PBE) show a decreasing of UE values in this order of basis sets and the opposite effect is observed for almost all the other functionals (except only for ωB97, M062X and M11 functionals when going from 6-31G(d,p) to 6-31+G(d,p) basis set). Although increasing the basis set reduces the error in the electron kinetic energy, the parameters in the semi-empirical correlation-exchange functionals are optimized for a certain basis set on a specific set of molecules, and the change of the latter leads to considerable deviations as observed in this study. This is confirmed further when more polarization functions are added to the 6-311+G(d,p) basis set because an increasing in the UE value for GGA functionals and the opposite effect for the other ones is always observed (to compare with MG3S see Figure S.1 in Supporting Information). In the analysis of the SE it was observed that all functionals except the GGA ones underestimate the reference values for the basis set 6-31+G(d,p) or larger. This underestimation could in principle be ascribed in the functionals which include HF exchange (from B3LYP in Table 1) to the HF contribution, which if consistent with the total electronic energy, would underestimate the reference value considerably for all basis sets studied. Local functionals (GGA) provide better agreement with reference values as the basis set size is augmented. One possible explanation is that larger basis sets would lead to a better, more homogeneous description of the molecular electronic density, especially for the most sensitive hydroxyl radical identified above. This is reflected in the larger decrease in SE or UE when diffuse-type functions on the oxygen atoms are added. The addition of one more Gaussian-type orbital in the valence shell through the triple-ζ basis sets leads to a smaller decrease of SE or UE in comparison. Range separated functionals (ωB97 family and M11 functional) are less sensitive to the flexibility of the basis set possibly due to the range separation of their non-local parts.

If the different functionals are compared for a given basis set, hybrid meta-GGA functionals do not perform better than the hybrid GGA. Semi-empirical functionals of the Minnesota family as M06, M06-2X or M05-2X, for example, perform as well as the ωB97X (with larger deviations for the M11 functional). Yet, no trends with the basis sets could be distinguished for this family of functionals, possibly due to their empirical construction and their high number of parameters. These parameters are optimized to reproduce reaction energies and other chemical properties in specific databases. Considering the M06 and the M06-2X functionals, for example, one observes smaller UE values for the latter. This functional was parameterized with databases that include transition states, which might be more representative of the homolytic bond dissociation process studied here and therefore explains the smaller errors [13].

The just discussed trends for SE and UE are maintained if the reaction enthalpy is calculated with each DFT method under the rigid rotor–harmonic oscillator approximation and compared to the experimental data (50.35 kcal mol^{-1}). The observed differences among methods are significant since the reported experimental error is only 0.10 kcal mol^{-1} (see Figures 2 and S.2 in the Supporting Information). These differences between functionals cannot be attributed at first glance only to the electronic structure method because here they might also arise from the error associated to the calculation of vibrational frequencies to obtain zero point energy and enthalpy approximations in combination with the assumption of the behavior as an ideal gas. However, at least 97% of the difference in SE value within a functional comes from variations in bond dissociation electronic energy (Table S.2 in the supporting information). The same is observed in the case of UE, except for the methods where the trend was not verified (ωB97, M062X and M11 functionals when going from 6-31G(d,p) to 6-31+G(d,p) basis set, as it was just stated). In general, zero point and thermal corrections were relatively insensitive to the electronic structure method as shown in Table S.2 of the supporting information. Therefore, trends in UE values with regard to experimental data can be mainly explained from arguments based on the electronic structure of hydrogen peroxide and hydroxyl radical, which enforces the study of the intrinsic factors for the Fenton reaction proposed in the introduction.

3.2 Electron affinity of the hydroxyl radical

Hydroxyl radical reduction (HRR) is the second reaction related to Fenton processes here studied. The inverse reaction energy equals the electron affinity of the hydroxyl radical, which was calculated by high-level ab-initio methods using complete basis set extrapolation (see Table 4). As in the case of the eBDE, the HF level of theory does not provide a good estimate of the electron affinity, due to the lack of Coulomb-type electron correlation between the unpaired electron in the hydroxyl radical and the added electron in the anion. Consequently, the MP2 correlation energy adds a large correction to the EA, while overestimating it by around 8 kcal mol^{-1}. Therefore in order to achieve a result of chemical accuracy, higher rank excitations in the cluster expansion are needed. The energy is well converged at the CCSDT(Q) level of theory with a correction of less than 0.5 kcal mol^{-1}. Finally, the CCSDT(Q)/CBS extrapolated value for the electron affinity (42.50 kcal mol^{-1}) nicely agrees with the experimental reference of 42.147 kcal mol^{-1}.

For the electron affinity the experimental data and the ab-initio CBS extrapolated value are very close and in principle both could be used as benchmark. We present here the comparison of EA values calculated with DFT functionals to the experimental reference value (Fig. 3) and the comparison to the ab-initio value is shown in the Figure S.3 in the supporting information.

Interestingly, all functionals show a negative value of SE, with exception of BLYP (a GGA type). The basis set dependence is very small for all functionals with no systematic deviation, as already observed by Hrusak et al. [44]. BLYP and PBE are very close to the experimental reference possibly due to error cancellation, and non-local functionals present an underestimation of EA. This underestimation has been related previously to the Hartree–Fock exchange in non-local functionals by Hrusak et al. [44]. The two meta-GGA functionals, MN12L and M06L, show the largest deviation. In general, functionals with HF exchange perform better than meta-GGA functionals but worse than GGA functionals. The inclusion of HF

Table 4 Contributions to the electronic electron affinity (EA) at various level of theory and basis sets and extrapolated to the CBS limit

EA (kcal mol^{-1})	SCF	MP2-SCF	CCSD-MP2	CCSD(T)-CCSD	CCSDT-CCSD(T)	CCSDT(Q)-CCSDT	Correlated EA
aug-cc-pvdz	− 4.98	49.89	− 10.24	2.94	− 0.03	0.42	37.60
aug-cc-pvtz	− 6.06	53.85	− 11.74	4.12	− 0.26	0.41	40.16
aug-cc-pvqz	− 6.20	55.47	− 12.24	4.38	–	–	41.42
aug-cc-pvQz	− 6.24	56.16	− 12.56	4.50	–	–	41.86
CBS limit	− 6.25	56.88	− 12.90	4.63	− 0.26	0.41	42.50

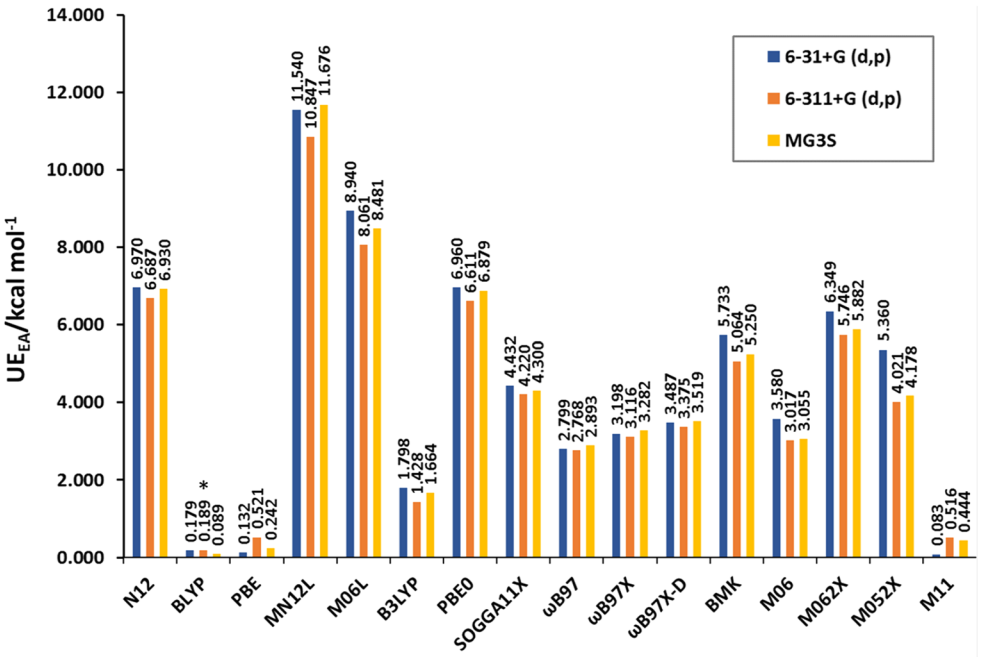

Fig. 3 Unsigned error (UE) for DFT calculated EA values compared to the experimental reference in kcal mol^{-1}. Signed errors (SE) are all negative, except for BLYP/6-311+G(d,p), which is marked with an asterisk. The same trend is verified when the ab-initio reference value is considered (see Figure S.3 in Supporting Information)

exchange in the BLYP and PBE functionals represented by B3LYP and PBE0 increase the UE value, possibly due to the poor performance of the HF method discussed above.

The family of the Minnesota functionals shows various performances. While MN12L showed the largest error, M11 exhibits the smallest. The errors for the rest of the functionals are in the range defined by M11 and MN12L. Notice that B3LYP (a HGGA-type) presents the second smallest UE values of the functionals, which is in agreement to the study of Hrusak etal. [44]. As already observed in the bond dissociation energy also here hybrid meta-GGA do not perform better than GGA.

Among the different functionals the ωB97X seems to provide the most consistent results considering the computational cost, although other functionals as PBE or BLYP predicted close values to the experimental data plausibly due to cancellation of errors.

3.3 Geometries of involved species

Besides the energetics it is also interesting to address whether different DFT functionals are able to reproduce the correct geometrical properties of hydrogen peroxide (only minor differences in the geometry were observed for the hydroxyl radical and its anion, as observed by Hrusak et al. [44], see Figures S.4 and S.5 in the supporting information). If a DFT functional is able to provide the correct geometry, the electronic energy could be calculated by ab-initio methods and, therefore, an accurate description of PBB and HRR reactions would become possible. The quality of the molecular geometries of hydrogen peroxide was addressed by comparing bond lengths, the oxygen–oxygen–hydrogen (OOH) angle and HOOH dihedral angle with experimental reference values. For the bond lengths all of the functionals present unsigned errors being lower than 0.045 Å (see Figures S.6 and S.7 in supporting information), whereas larger variations are observed for the angles.

The deviations from the experimental value for the HOO angle and the HOOH dihedral angle are shown in Figs. 4 and 5, respectively (full data in Figures S.8 and S.9 in the supporting information). The deviation of the OOH angle clearly separates the non-empirical GGA functionals from the semi-empirical MN12L and the meta-GGA functionals. PBE and BLYP provide negative deviation for the angles, whereas the other present positive deviation in the same range of one or two degrees. However, for the GGA functionals the absolute deviation gets smaller with increasing the basis set's size, which might, again, be related to a better and more homogeneous description of the electron density. For the other functionals, which result in structures with angles larger than the experimental value, the deviation increases with the basis set. Addition of diffuse functions increases for almost all functionals the deviation by more than 50%. Extending the valence shell of the basis set resulting in the 6-311+G(d,p) basis set improves the angles for non-empirical GGA functionals but increases slightly the error, as also observed for the extra polarization-type functions.

For the HOOH dihedral angle the tendency of the different functionals is not clear. Some GGA functionals lead to a positive deviation and other to a negative one. Increasing the basis set with diffuse function or more Gaussian functions in the valence shell always leads to

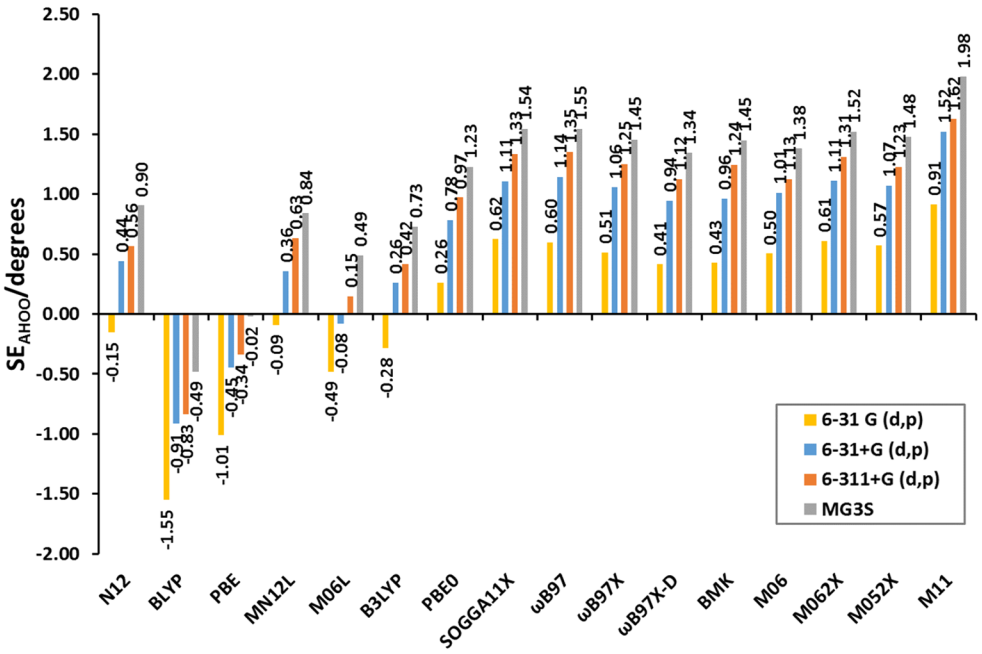

Fig. 4 Signed error (SE) in degrees for DFT calculated HOO angles in hydrogen peroxide with regard to the experimental reference value

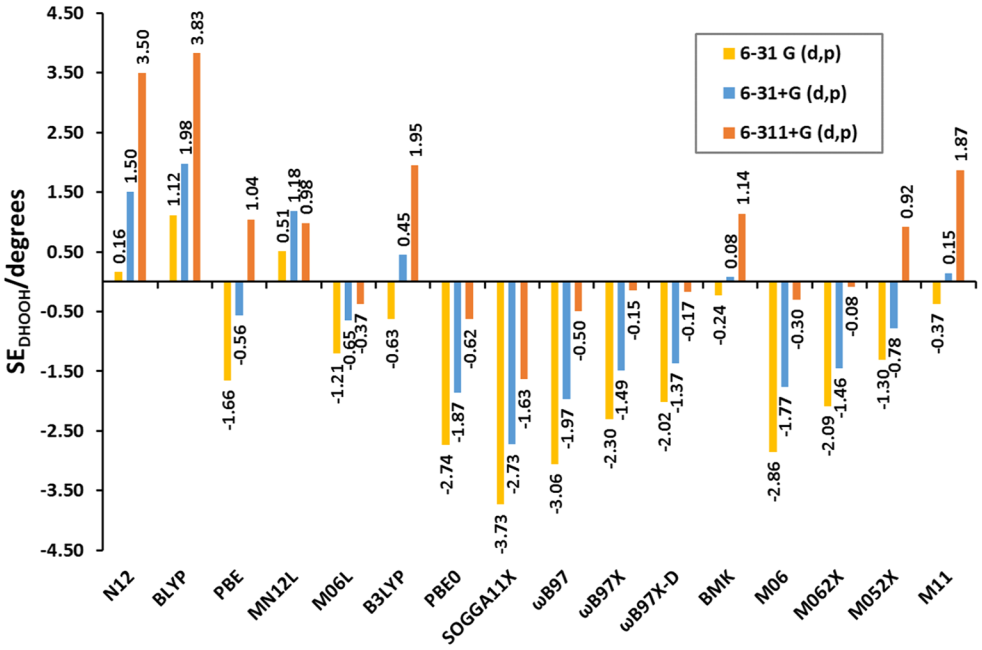

Fig. 5 Signed error (SE) in degrees for DFT calculated HOOH dihedral angle in hydrogen peroxide with regard to the experimental reference value. MG3S basis showed a highly negative deviation in all the tested functionals, which is shown in figure S.9

larger dihedral angles except for the empirical MN12L GGA functional. Here, the effect of an extra basis function in the valence shell of the oxygen atom has a large effect in the dihedral angle. For the functionals including HF exchange the 6-311+G(d,p) basis set provides angles which are very close to the experimental value independently of the functional used, except for B3LYP which overestimates its value. This trend is not so clear for the empirical functionals from the Minnesota family, where the larger basis set overestimates its value as observed for the M11 or M05-2X.

When both angles are considered, it is observed that an increasing in the basis set leads in general to more extended HOO and HOOH angles, probably because the system must compensate the increase in Coulombic repulsion with an extension in the angle. On the other hand, no combination of functional and basis set seems to provide the best result in both cases. Hybrid functionals lead to larger absolute deviation in the OOH angle but smaller errors in the HOOH dihedral angle. In general, it is difficult to conclude which functional/basis set combination should be used for the correct geometry. However, considering the computational cost the PBE functional seems to be a suitable candidate for the calculation of geometries in hydrogen peroxide, since with the 6-31+G(d,p) basis set the obtained deviations are below 1 degree. Other candidates are MN12L and M06L functionals together with the B3LYP/6-31+G(d,p) method. The fact that MN12L and M06L provide a good geometry for hydrogen peroxide might be originated to the fact that this molecule was present in the database used to optimize the parameter set of these functionals [12, 13].

4 Conclusions

Two reactions related to Fenton processes and associated with the homolytic bond dissociation energy of the peroxide bond in hydrogen peroxide (BDE) and the electron affinity (EA) of the hydroxyl radical have been studied with high-accuracy extrapolated ab-initio methods. The obtained results are in perfect agreement with the experimental reported values and assign a large contribution of the electron correlation energy to the electronic energy associated with both processes. The contribution of the electron correlation energy only converges to chemical accuracy of 1.0 kcal mol^{-1} at the CCSDT(Q) level.

DFT-based methods provide bond dissociation electronic energies and electron affinities which are significantly better than HF and comparable to the MP2 or CCSD level of theory. The inclusion of HF exchange in the functional (functionals below B3LYP in Table 1) leads in general to a decreasing of BDE and EA, which may be related to the underestimation of the HF results at the CBS limit (Tables 3 and 4). This trend can be analyzed together with the basis set dependence observed in the results of the BDE values. Extending the basis set induces a less absolute deviation for BDE in GGA functionals. For example, N12 and BLYP functionals yield UE values under 1.00 kcal mol^{-1} in combination with the 6-311+G(d,p) basis set, but this absolute deviation reaches 6.00–8.00 kcal mol^{-1} when the 6-31G(d,p) basis set is considered with regard to the ab-initio reference. The opposite effect is observed for non-local functionals, where UE values become larger as the basis set is extended. For example, the popular B3LYP functional yields an UE value of 1.06 kcal mol^{-1} with the 6-31G(d,p) basis set, but

it increases up to 6.60 kcal mol^{-1} for 6-311+G(d,p). Therefore, non-local functionals are better combined with smaller basis sets with UE values around 1.00 kcal mol^{-1} reducing the computational cost. On the other hand, more local functionals require larger basis sets in order to reach similar UE values, probably due to the better modeling of the electronic density when the basis set is extended (Fig. 1). Hybrid Meta-GGA functionals from the Minnesota family do not perform better than hybrid GGA. For DFT calculated EA values no systematic behavior with regard to the basis set is observed. MN12L, M06L and PBE0 functionals show, however, high UE values (over 6.60 kcal mol^{-1}) whereas BLYP, PBE and M11 yield electron affinities very close to the experimental reference value (Fig. 3) probably due to an error cancellation. From all functionals studied the range separated with short range exchange ωB97X hybrid functional combined with the 6-31+G(d,p) basis set is the best combination for these two reactions due to its low computational cost and since its errors present smaller dependence on the basis set.

Analysis of geometries obtained with the different DFT methods for the involved species shows that most functionals provide reasonable geometries with error in the bond lengths below 0.05 Å and in the angles between one and two degrees. Increasing the basis set leads in general to higher values of both angles, probably due to the compensation of additional Coulombic repulsion arising from the inclusion of more electronic density in the bond region (Figs. 4 and 5). When this fact is analyzed in conjunction with the features of the functionals, it can be concluded that the non-empirical ones (BLYP and PBE) needed larger basis sets in order to provide small absolute deviations for the angle HOO. The PBE functional yields an UE value of 0.02° with the MG3S basis set, but it increases up to 1.55° for 6-31G(d,p). The opposite effect is verified in the semi-empirical functionals: absolute deviation for the angle HOO increases from 0.62° up to 1.54° for the SOGGA11X functional with increasing basis set (Fig. 4). Although the results of the dihedral angle in hydrogen peroxide do not show the same systematic dependence of the basis set, for both angles the best geometries are achieved with the M06L, MN12L or B3LYP functionals and the 6-31+G(d,p) basis set.

Although no systematic behavior of DFT methods was observed in the different assayed parameters, this constitutes an expected result because of the nature of the Density Functional Theory, which does not follow, for example, a variational philosophy [25–28]. However, this fact strongly justifies the need for performing this benchmark study as a good starting point toward a theoretical description of reactions were hydrogen peroxide is involved (e.g. the Fenton reaction). Therefore, this study may be used in the future to balance computational cost and accuracy in the theoretical characterization of other aspects of this kind of reactions, for instance, the inclusion of transition metals or other substituted peroxide molecules.

Acknowledgements D. Carmona acknowledges CONICYT for the doctoral scholarship 21131021. O.A.D.-G. thanks Fondo Nacional de Desarrollo Cientifico y Tecnologico (Fondecyt) for his postdoctoral fellowship No. 3170029. E.V.-M. acknowledges financial support by Fondecyt through grant 1160197 and the Max-Planck-Society through a Max-Planck-Partner group.

References

1. Bokare AD, Choi W (2014) J Hazard Mater 275:121
2. Prousek J (2007) Pure Appl Chem 79(12):2325
3. Fenton HJH (1894) J Chem Soc Trans 65:899
4. Luo YR (2007) Comprehensive handbook of chemical bond energies. CRC Press, Boca Raton
5. Gold Book (2014) IUPAC, 528
6. Cramer CJ, Truhlar DG (2009) Phys Chem Chem Phys 11:10757
7. Yepes D, Seidel R, Winter B, Blumberger J, Jaque P (2014) J Phys Chem B 118(24):6850
8. Peverati R, Truhlar DG (2012) J Chem Theory Comput 8(7):2310
9. Becke AD (1988) Phys Rev A 38(6):3098
10. Lee C, Yang W, Parr RG (1988) Phys Rev B 37(2):785
11. Perdew JP, Burke K, Ernzerhof M (1996) Phys Rev Lett 77(18):3865
12. Peverati R, Truhlar DG (2012) Phys Chem Chem Phys 14(38):13171
13. Zhao Y, Truhlar DG (2008) Theor Chem Acc 120(1–3):215
14. Stephens P, Devlin F, Chabalowski C, Frisch MJ (1994) J Phys Chem 98(45):11623
15. Adamo C, Barone V (1999) J Chem Phys 110(13):6158
16. Peverati R, Truhlar DG (2011) Communication: a global hybrid generalized gradient approximation to the exchange-correlation functional that satisfies the second-order density-gradient constraint and has broad applicability in chemistry. J Chem Phys 135(19):191102
17. Chai JD, Head-Gordon M (2008) J Chem Phys 128(8):084106
18. Chai JD, Head-Gordon M (2008) Phys Chem Chem Phys 10(44):6615
19. Boese AD, Handy NC (2001) J Chem Phys 114(13):5497
20. Zhao Y, Schultz NE, Truhlar DG (2006) J Chem Theory Comput 2(2):364
21. Peverati R, Truhlar DG (2011) J Phys Chem Lett 2(21):2810
22. Roothaan CCJ (1951) Rev Mod Phys 23(2):69
23. Møller C, Plesset MS (1934) Phys Rev 46(7):618
24. Peverati R, Truhlar DG (2014) Philos Trans R Soc A 372(2011):20120476
25. Kümmel S, Kronik L (2008) Rev Mod Phys 80:3
26. Dykstra C, Frenking G, Kim K, Scuseria G (2005) Theory and applications of computational chemistry: the first forty years. Elsevier, Amsterdam
27. Parr RG, Yang W (1989) Density-functional theory of atoms and molecules. Oxford University Press, New York
28. Kohn W, Sham LJ (1965) Phys Rev 140:A1133
29. Becke AD (1989) Density functional theories in quantum chemistry: beyond the local density approximation. ACS Publications, Washington
30. Perdew JP, Schmidt K (2001) Jacob's ladder of density functional approximations for the exchange-correlation energy. In: AIP conference proceedings, AIP vol 577, p 1
31. Savin A, Colonna F, Pollet R (2003) Int J Quantum Chem 93(3):166

32. Harris J (1984) Phys Rev A 29(4):1648
33. Leininger T, Stoll H, Werner HJ, Savin A (1997) Chem Phys Lett 275(3–4):151
34. Lee AM, Taylor SW, Dombroski JP, Gill PMW (1997) Phys Rev A 55:3233
35. Smith JR, Kim JB, Lineberger WC (1997) Phys Rev A 55:2036
36. Huber KP (2013) Molecular spectra and molecular structure: IV. Constants of diatomic molecules, Springer, Berlin
37. Rosenbaum NH, Owrutsky JC, Tack LM, Saykally RJ (1986) J Chem Phys 84(10):5308
38. Baraban JH, Changala PB, Stanton JF (2018) J Mol Spectrosc 343:92
39. Parrish RM, Burns LA, Smith DGA, Simmonett AC, DePrince AE, Hohenstein EG, Bozkaya U, Sokolov AY, Di Remigio R, Richard RM, Gonthier JF, James AM, McAlexander HR, Kumar A, Saitow M, Wang X, Pritchard BP, Verma P, Schaefer HF, Patkowski K, King RA, Valeev EF, Evangelista FA, Turney JM, Crawford TD, Sherrill CD (2017) J Chem Theory Comput 13(7):3185
40. Kállay M, Rolik Z, Csontos J, Ladjánszki I, Szegedy L, Ladóczki B, Samu G, Petrov K, Farkas M, Nagy P et al (2016) http://www.mrcc.hu. Accessed 26 Aug
41. Frisch MJ, Trucks GW, Schlegel HB, Scuseria GE, Robb MA, Cheeseman JR, Scalmani G, Barone V, Mennucci B, Petersson GA, Nakatsuji H, Caricato M, Li X, Hratchian HP, Izmaylov AF, Bloino J, Zheng G, Sonnenberg JL, Hada M, Ehara M, Toyota K, Fukuda R, Hasegawa J, Ishida M, Nakajima T, Honda Y, Kitao O, Nakai H, Vreven T, Montgomery JA Jr, Peralta JE, Ogliaro F, Bearpark M, Heyd JJ, Brothers E, Kudin KN, Staroverov VN, Kobayashi R, Normand J, Raghavachari K, Rendell A, Burant JC, Iyengar SS, Tomasi J, Cossi M, Rega N, Millam JM, Klene M, Knox JE, Cross JB, Bakken V, Adamo C, Jaramillo J, Gomperts R, Stratmann RE, Yazyev O, Austin AJ, Cammi R, Pomelli C, Ochterski JW, Martin RL, Morokuma K, Zakrzewski VG, Voth GA, Salvador P, Dannenberg JJ, Dapprich S, Daniels AD, Farkas O, Foresman JB, Ortiz JV, Cioslowski J, Fox DJ (2009) Gaussian 09 revision E.01. Gaussian Inc., Wallingford
42. Lynch BJ, Zhao Y, Truhlar DG (2003) J Phys Chem A 107(9):1384
43. Lee TJ, Schaefer HF III (1985) J Chem Phys 83(4):1784
44. Hrušák J, Friedrichs H, Schwarz H, Razafinjanahary H, Chermette H (1996) J Phys Chem 100(1):100